HIGH EFFICIENCY MULTI-JUNCTION SPACE SOLAR DEVELOPMENT UTILIZING LATTICE GRADING

Mark A. Stan, Victor G. Weizer, AnnaMaria Pal, Linda M. Garverick, Osman Khan, and Samar Sinharoy
Essential Research, Inc., Cleveland, OH 44135

Richard W. Hoffman, Jr., Phillip P. Jenkins, and David A. Scheiman
The Ohio Aerospace Institute, Cleveland, OH 44135

Navid S. Fatemi
EMCORE PhotoVoltaics
Albuquerque, NM 87123

Abstract

Progress towards achieving a high one-sun air mass 0 (AM0) efficiency in a monolithic dual junction solar cell comprised of a 1.62 eV InGaP top cell and a 1.1 eV InGaAs bottom cell grown on buffered GaAs is reported. The performance of stand-alone 1.62 eV InGaP and 1.1 eV InGaAs cells is compared to that of the dual junction cell. Projected AM0 efficiencies of 15.7 % and 16.5 % are expected for the 1.62 eV InGaP and 1.1 eV InGaAs cells grown on buffered GaAs. The dual junction cell has a projected one-sun AM0 conversion efficiency of 17 %. The projected efficiencies are based upon the application of an optimized anti-reflective coating (ARC) to the as-grown cells. Quantum efficiency (QE) data obtained from the dual junction cell indicate that it is bottom cell current limited with the top cell generating 50 % more current than the bottom cell. A comparison of the QE data for the stand-alone 1.1 eV InGaAs cell to that of the 1.1 eV InGaAs bottom cell in the tandem configuration indicates a degradation of the bottom cell conversion efficiency in the tandem configuration. The origin of this performance degradation is at present unknown. If the present limitation can be overcome, then a one-sun AM0 efficiency of 26 % is achievable with the 1.62 eV/1.1 eV dual junction cell grown lattice-mismatched to GaAs.

Introduction

Theoretical predictions of the solar conversion efficiency of multi-junction solar cells show that the maximum conversion efficiency occurs for devices whose bandgaps are such that they are not lattice-matched to substrates of binary III-V compounds. Consequently, a trade-off between choosing compounds with optimized bandgaps or compounds that lattice match to binary III-V substrates must be made. The traditional approach has been to utilize compounds that are lattice-matched to the underlying substrate. [1] In this approach one avoids misfit and threading dislocation formation. Such defects have been shown to introduce trapping centers. [2]

The dual junction monolithic space solar cell presently used in production consists of an $InGaP_2$ top cell lattice-matched to a GaAs bottom cell. Modeling shows that this design will yield a one-sun air mass 0 (AM0) efficiency of 28.6%. [3] The highest efficiency reported to date with this archetypal cell design is 26.9%. If, however, one relaxes the constraint of lattice matching, then an upper limit efficiency of nearly 32.5% is possible in a dual junction configuration. This efficiency is theoretically possible in a tandem design that utilizes a 1.75 eV top cell and a 1.1 eV bottom cell. Recently, a one-sun AM0 efficiency of 21.6% has been reported in a design that uses a 1.65 eV InGaP top cell and a 1.18 eV InGaAs bottom cell grown lattice-mismatched to GaAs. [4] Further improvements in the efficiency are possible by thinning the top cell. Quantum efficiency measurements indicate that the top cell generated 24% more current than did the bottom cell under one-sun AM0 illumination.

Our approach to space solar cell design is based upon optimizing the dual junction cell in terms of bandgap. [5] This method allows one to achieve current matching of the top and bottom cells without resorting to thinning of the top cell. The 1.75 eV bandgap top cell lattice-matched to the underlying 1.1 eV InGaAs bottom cell requires the quaternary compound InGaAlP. As a first step in our process development we have chosen to grow a tandem cell using a 1.62 eV InGaP ternary top cell latttice-matched to a 1.1 eV InGaAs bottom cell. In this paper we present performance data for the dual junction components: a 1.1 eV n/p InGaAs cell, a 1.62 eV n/p InGaP cell, a 1.1 eV p++/n++ tunnel junction interconnect, and the complete 1.62 eV/1.1 eV n/p dual junction cell.

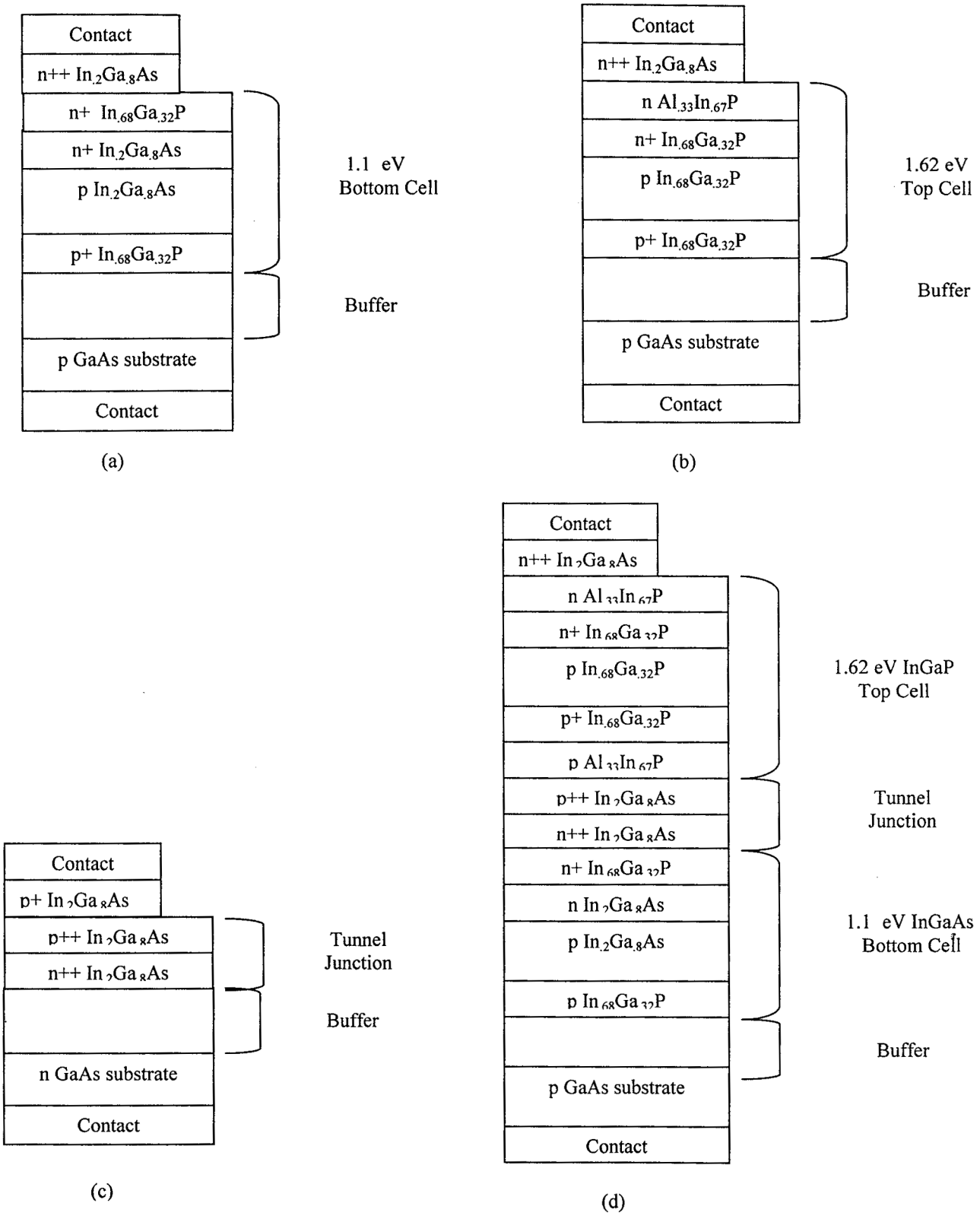

Figure 1. Epilayer structures for the 1.1 eV n/p InGaAs, 1.62 eV n/p InGaP, 1.1 eV p++/n++ InGaAs tunnel junction test structure, and the 1.62 eV InGaP/ 1.1 eV InGaAs dual junction cells are shown in (a), (b), (c), and (d) respectively.

Device Fabrication and Evaluation

The device epilayers were grown using low pressure organometallic vapor phase epitaxy (LP-OMVPE) in a horizontal reactor. All layers were grown at 150 torr on (100) GaAs substrates with 2° off cut to the nearest <110> direction or a 6° off cut to the <111>B direction. The growth rate was 7 um/hr and 4.4 um/hr for the InGaAs and InGaP cells, respectively. Precursors used for the growth were trimethylgallium (TMGa), trimethylindium (TMIn), pure arsine, pure phosphine, diethylzinc (DEZn), and diluted silane in hydrogen. Each of the devices is fabricated with a proprietary buffer layer structure whose purpose is to grade the lattice parameter from GaAs (5.6532 Å) to that of $In_{.2}Ga_{.8}As$ (5.736 Å). The buffer layer structure is designed to prevent threading dislocations from reaching the active area of the solar cells. Transmission electron microscopy (TEM) was used to determine defect structure related to lattice mismatch and to estimate the dislocation defect densities. Typically, if one defect is observed in the TEM field of view, then the defect density is above $1x10^7$ cm^{-2}. No dislocation defects were observed in the active area of any of the solar cell structures. High-resolution x-ray diffraction (HRXRD) was used to determine composition and lattice matching of the InGaAs and InGaP alloys. The InGaAs and InGaP epilayers have [004] reflection full width at half maximum (FWHM) values of approximately 250 arc-sec. In addition, all epilayers above the buffer structure are lattice-matched to one another to within 100 arc-sec.

Fig. 1 contains a schematic diagram of each of the devices discussed in this paper. The 1.1 eV bottom cell shown in Fig. 1 (a) is comprised of a 0.5 um n+ $In_{.2}Ga_{.8}As$ emitter, a 3.0 um p $In_{.2}Ga_{.8}As$ base and a 0.05 um $In_{.68}Ga_{.32}P$ window layer. The 1.62 eV bottom cell shown in Fig. 1 (b) is comprised of a 0.05 um n+ $In_{.68}Ga_{.32}P$ emitter, a 1.5 um p $In_{.68}Ga_{.32}P$ base, a 0.05 um p+ $In_{.68}Ga_{.32}P$ back surface field, and a 0.05 um n $Al_{.33}In_{.67}P$ window layer. A p++/n++ $In_{.2}Ga_{.8}As$ tunnel junction test structure, shown in Fig. 1 (c), with the same thickness (0.05 um) and doping levels ($1x\ 10^{19}$ $/cm^3$) used in the dual junction was evaluated prior to it's incorporation in the dual junction. The dual junction cell shown in Fig 1 (d) combines the components of each of the subcells and connects them together with the $In_{.2}Ga_{.8}As$ tunnel junction. We have chosen to use InGaAs as the tunnel junction interconnect compound since it is easily degenerately doped. The use of InGaAs as the subcell interconnect results in some absorption of red light that the bottom cell is designed to convert. As such, we plan to use a higher bandgap compound as the tunnel junction interconnect material in future designs.

Vacuum evaporated gold-based metallization was used for front and rear contacts. The front grid was fabricated using reverse image photolithography and lift off techniques. Individual cells were isolated by mesa etching into cell areas of 1 cm^2 with a grid shadow of 5%. AM0 conversion efficiencies were measured at 25°C using a single source, Spectrolab X25 solar simulator at the NASA Glenn Research Center in Cleveland, OH. Spectral response measurements as well as reflectance measurements were performed on each of the cells in order that the internal quantum efficiency could be determined.

The light current-voltage (I-V) of a 1.1 eV InGaAs bottom cell is show in Fig. 2. The one-sun AM0 efficiency of 12.56%, open circuit voltage V_{oc} = 764 mV, short circuit current density J_{sc} = 26.8 mA/cm^2, and fill factor FF= 78.6% indicate the high quality of this InGaAs cell grown mismatched to GaAs. We expect that this cell would have a one-sun AM0 efficiency of 16.5% with an optimized anti-reflective coating (ARC).

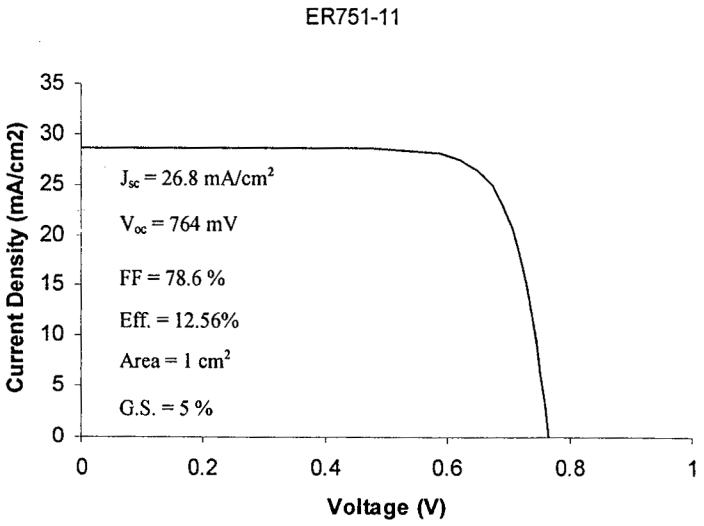

Figure 2. Current-voltage characteristic of a 1 sq. cm. 1.1 eV n/p InGaAs/ GaAs solar cell under AM0, one-sun illumination.

To put this performance into perspective, one need only to compare these data to that of a planar Si solar cell. The one-sun AM0 efficiency, open circuit voltage, and fill factor for high quality Si are 15%, 615 mV, and 81% respectively. [6] Our 1.1 eV cell performance indicates the effectiveness of the proprietary buffer in localizing the dislocation defects away from the active area of the cell.

The internal quantum efficiency of the 1.1 eV n/p InGaAs solar cell is shown in Fig.3. This data was obtained from the measured external quantum efficiency (EQE) and the optical reflectance in same wavelength interval. The optical reflectance measurements were performed on the fully processed cell and the data were not corrected for additional reflection

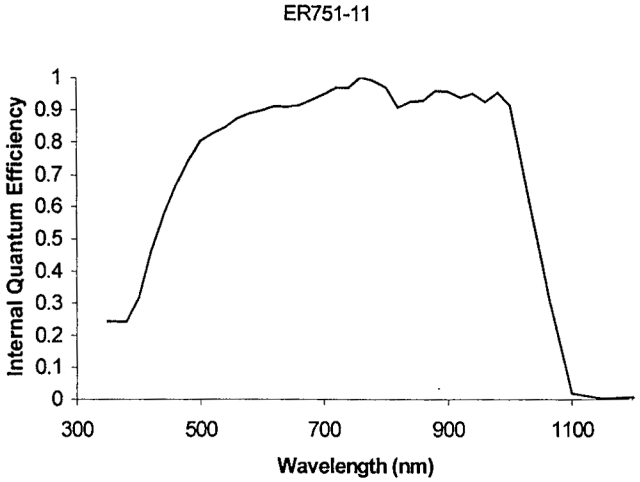

Figure 3. Internal quantum efficiency of a 1 sq. cm. 1.1 eV n/p InGaAs/ GaAs solar cell.

from the Au contact metallization. The most important portion of the IQE characteristic of the InGaAs cell lies between the 1100 nm absorption edge of the InGaAs and the 765 nm absorption edge of the InGaP. Within that wavelength band the IQE magnitude is $\geq$ 0.9. This cell performance is typical of the best 50% of the devices on a 2" diameter wafer.

The light I-V of a 1.62 eV n/p $In_{.68}Ga_{.32}P$ solar cell is shown in Fig. 4. The one-sun AM0 efficiency of 11.56%, V_{oc} = 1.13 V, J_{sc} = 17.0 mA/cm^2, and FF= 82.4% represents the best cell performance on this particular wafer. However 50 % of the devices had one-sun AM0 efficiencies in excess of 11%. We expect that this cell will demonstrate a one-sun AM0 efficiency of 15.7% and a J_{sc} = 22.4 mA/cm^2 with an optimized ARC.

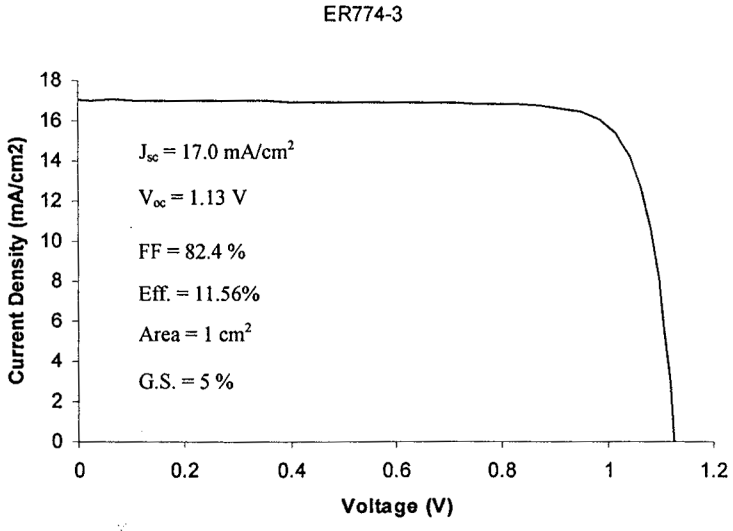

Figure 4. Current-voltage characteristic of a 1 sq. cm. 1.62 eV n/p InGaP solar cell under AM0, one-sun illumination.

The internal quantum efficiency of this cell shown in Fig. 5 is quite good, however there is a rather abrupt fall off in the IQE below 590 nm. Reflectance of this material has been performed and it is essentially flat in the wavelength region about 590 nm. The position of the transition in the IQE at 590 nm correlates well with the absorption edge of the $Al_{.33}In_{.67}P$ surface passsivation layer. In fact, this feature can be seen in the QE data of the dual junction cell grown by the Fraunhofer group. [4]

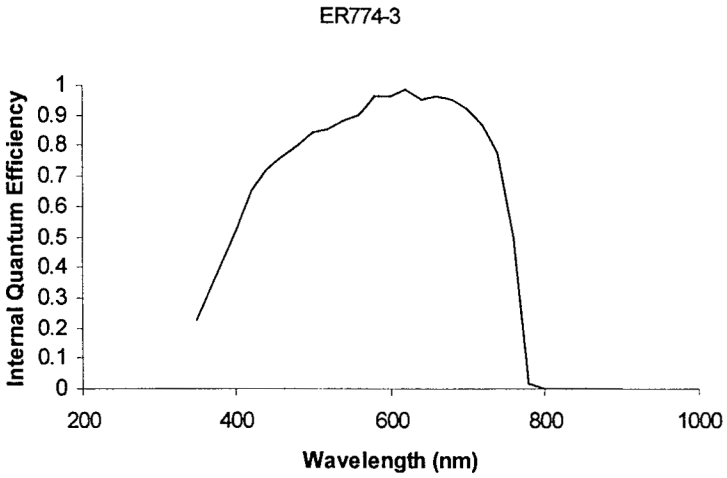

Figure 5. Quantum efficiency of a 1 sq. cm. 1.62 eV n/p InGaP solar cell.

They use a 0.03 um thick AlInP as the front surface passivation layer. This suggests that our $Al_{.33}In_{.67}P$ passivation layer thickness should be decreased from the present value of 0.05 um. Further improvements in the InGaP top cell may be realized by thinning the top cell such that the open circuit voltage may increase as a consequence of reducing the bulk recombination currents.

The structure shown in Fig. 1 (c) was processed into 150 um dia. circular diodes to evaluate the p++/n++ $In_{.2}Ga_{.8}As$ compound as a tunnel junction interconnect. Junction thicknesses of 0.1um and 0.05 um were evaluated. The peak-to-valley currents were found to be independent of the junction thickness whereas the peak voltage increased with decreasing junction thickness. A typical I-V characteristic of a 0.05 um thick tunnel junction is shown in Fig. 6. The junction was grown on the proprietary buffer layer to roughly simulate the conditions in a dual junction configuration. The device is characterized by a peak tunneling current density of 750 mA/cm^2 and a series resistivity of .1 ohm-cm^2 at the expected operating current density of 20 mA/cm^2. This tunnel junction series resistance will result in a negligible voltage drop at the dual junction operating current.

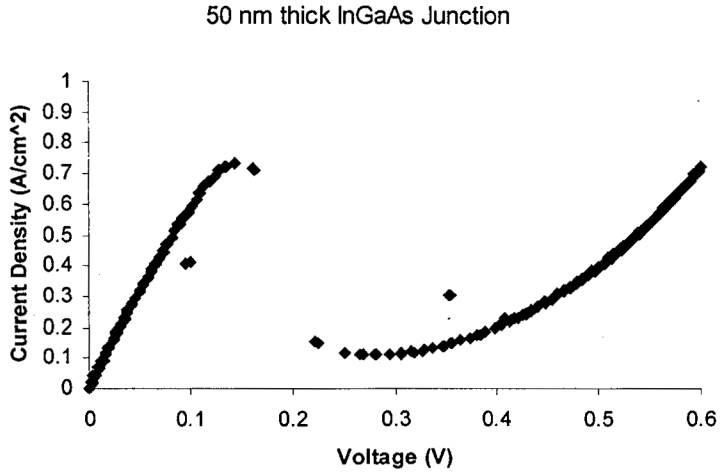

Figure 6. Current-voltage characteristic of a 150 um dia. 1.1 eV p++/n++ $In_{.2}Ga_{.8}As$ tunnel diode.

Shown in Fig. 7 is the light I-V characteristic of a 1.62 eV/1.1 eV n/p dual junction cell. The cell is characterized by a V_{oc} = 1.77 V, a J_{sc} = 11.9 mA/cm^2, a FF = 84.1%, and a one-sun AM0 efficiency of 12.9%. The AM0 efficiency of our dual junction cell would be 17% with an optimized ARC. The predicted efficiency of a 1.62 eV/1.1 eV n/p dual junction cell is 27.0 %. The short fall in the AM0 efficiency is a consequence of lower than expected V_{oc} and J_{sc} values. The dual junction V_{oc} is ≅100 mV less than the sum of the V_{oc} 's of the best 1.1 eV InGaAs and 1.62 eV InGaP cells. The origin of this voltage difference may be due to a degradation of the InGaP top cell base layer as a result of Zn out diffusion from the InGaAs tunnel junction. Secondary ion mass spectroscopy (SIMS) analysis of the cell is required to confirm this. Similar observations have been made in the lattice-matched

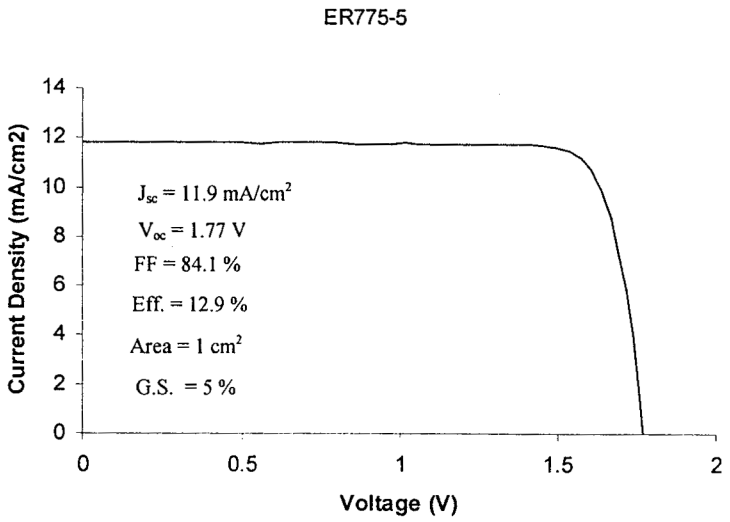

Figure 7. Current-voltage characteristic of a 1 sq. cm. 1.62 eVn/p $In_{.68}Ga_{.32}P$/ 1.1 eV $In_{.2}Ga_{.8}As$ dual junction cell.

$InGaP_2$/GaAs dual junction cell. [7] In that case the problem was solved with the use of C doping instead of Zn doping. In fact, the Fraunhofer group [4] uses C doped AlGaAs in their InGaP/InGaAs design and they report a V_{oc} /E_g ratio of 0.69 where E_g is the sum of the bandgaps of the dual junction subcells. The V_{oc} /E_g ratio for our dual junction cell is 0.65. These facts are consistent with the hypothesis of Zn dopant diffusion into the InGaP cell base acting to increase the dark current in our dual junction cell. If we are able to design a dual junction cell with no V_{oc} loss i.e. V_{oc} = 1.89 V then we would have a dual junction cell with an 18.5 % one-sun AM0 efficiency.

In addition to a lower than expected V_{oc}, the dual junction J_{sc} is only 70% of the value of the stand-alone 1.62 eV top cell. As such, the dual junction device is bottom cell current limited. The IQE for the 1.62 eV n/p InGaP/ 1.1 eV n/p InGaAs dual junction is shown in Fig. 8 along with the IQE data of the 1.1 n/p $In_{.2}Ga_{.8}As$ cell from Fig. 3 and the IQE data of the 1.62 eV n/p $In_{.68}Ga_{.32}P$ cell from Fig. 5. Integration of the QE data of the top and bottom subcells indicates that the top cell is generating 50% more current than the bottom cell. The bottom cell IQE data in Fig. 8 indicates that for this subcell the performance is not the same in the stand-alone and dual junction configurations. In particular, the magnitude of the bottom cell QE is 15% lower in the dual junction configuration. As mentioned previously, we expected some absorption of the light for wavelengths beyond 765nm. Computer modeling of absorption due to the presence of a lightly doped 0.05 um thick InGaAs layer indicates that a 7% reduction of the bottom cell J_{sc} would result. This reduction is far short of the measured 50 % reduction. Possible explanations for the reduced QE in the bottom cell could be a high interface recombination velocity at the InGaP window/ InGaAs emitter interface or a short diffusion length in the InGaAs emitter. Perhaps these effects are due to the presence of the tunnel junction. An experiment in which the QE of the tandem cells is measured after the InGaP top cell and InGaAs tunnel junction are removed via wet etching should allow one to determine if the reduced QE observed in the InGaAs bottom cell is a result of absorption in the InGaAs tunnel junction or a defective InGaAs bottom cell. Computer modeling indicates that the InGaAs bottom cell should produce 22 mA/cm^2 under one-sum AM0 illumination in the dual junction configuration. As such, the bottom cell is generating only 75 % of the current that it is predicted to produce.

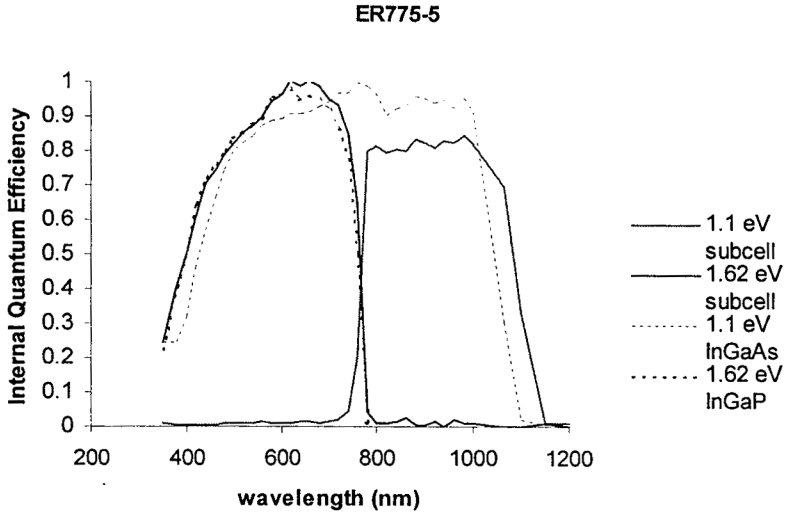

Figure 8. Internal quantum efficiency of a 1 sq. cm. 1.62 eV n/p InGaP/ 1.1 eV InGaAs dual junction cell, a 1 sq. cm. 1.62 eV n/p InGaP single junction cell, and a 1 sq. cm. 1.1 eV InGaAs single junction cell.

If a dual junction cell can be fabricated with a thinned top cell having the same quality top cell characteristics as those shown in Fig. 4 one can expect a dual junction efficiency as high as 26 %. A possible low absorption structure for the tunnel junction may be a C doped AlGaAs emitter and a Si doped InGaP base. Finally, the use of the InGaAlP quaternary for a 1.75 eV top cell in the dual junction design is necessary in order to achieve the highest conversion efficiency in the mismatched solar cell structure.

Summary

We have grown 1.1 eV n/p InGaAs cells, 1.62 eV n/p InGaP cells, and 1.62 eV n/p InGaP / 1.1 eV n/p InGaAs dual junction cells. Given an optimized ARC, the projected one-sun AM0 efficiencies of those cells are 16.5 %, 15.7 %, and 17.0 % respectively. A comparison of the dual junction V_{oc} with that of the individual 1.62 eV InGaP and 1.1 eV InGaAs cells indicates that the present dual junction design has an enhanced dark current leading to a V_{oc} loss. A similar comparison of the J_{sc} data indicates a loss of conversion efficiency in the InGaAs bottom cell. Additional experiments are necessary to determine the origin of the InGaAs bottom cell degredation in the dual junction configuration. Despite these difficulties, our results indicate that a 26 % one-sun AM0 efficiency can be obtained by controlling the dual junction dark currents, the tunnel junction optical losses, and employing top cell thinning.

This work was supported by the NASA Glenn Research Center under SBIR contract NAS3-98026.

References

[1] J.M. Olson, S.R. Kurtz, A.E. Kibbler, and P. Faine, Appl. Phys. Lett., 56, 623 (1990).
[2] D. Pal, E. Gombia, R. Mosca, A. Bosacchi, and S. Franchi, J. Appl. Phys., 84, 2965 (1998).
[3] J.C.C. Fan, B-Y. Tsaur, and B.J. Palm, Proc. 16th IEEE Photovoltaic Specialists Conf., 692 (1982).
[4] F. Dimroth, U. Schubert, and A.W. Bett, preprint submitted to the J. Appl. Phys. (1999).
[5] R.W. Hoffman, N.S. Fatemi, M.A. Stan, P. Jenkins, V.G. Weizer, D.A. Scheiman, and D.J. Brinker, Proc. of the Fall Meeting of the Materials Research Society, Boston MA, Nov. 30-Dec. 4, 1998.
[6] *Solar Cells and their Applications,* edited by L. D. Partain, (John Wiley and Sons, New York 1995), p. 25.
[7] K.A. Bertness, S. R. Kurtz, D.J. Friedman, A.E. Kibbler, C. Kramer, J.M. Olson, Appl. Phys. Lett., 65, 989 (1994).